UNIVERSITY OF TEXAS AT SAN ANTONIO
San Antonio, Texas

PHOTOPHYSICAL STUDY OF THE INTERACTIONS AND INFLUENCE ON TUBULIN POLYMERIZATION: PORPHYRINS VS. ANTI-MICROTUBULE AGENTS

A Thesis Submitted in Partial Fulfillment of the Requirements for
the Bachelor of Science Degree in Physics
with Tier 2 Honors in the Honors College

Eric M. Johnson

Department of Physics and Astronomy
December 2006

PREPARED BY:

Eric M. Johnson

APPROVED BY:

Dr. Lorenzo Brancaleon, Thesis Advisor

Dr. Chonglin Chen, Thesis Reader

Dr. Dhiraj Sardar, Thesis Reader

Dr. Richard Diem, Dean of the Honors College

RECEIVED BY THE HONORS COLLEGE

December 2007

PREPARED BY:



Eric M. Johnson

APPROVED BY:



Dr. Lorenzo Brancaleon, Thesis Advisor

Dr. Chonglin Chen, Thesis Reader



Dr. Dhiraj Sardar, Thesis Reader

Dr. Richard Diem, Dean of the Honors College

RECEIVED BY THE HONORS COLLEGE

December 2007

Abstract

Studies suggest that irradiation of porphyrins produces direct damage of proteins including tubulin. Our previous fluorescence spectroscopy investigation of the interaction of meso-tetra(4-sulfonatephenyl)porphine ($TPPS_4$) and protoporphyrin IX (PPIX) with tubulin showed that binding to the protein occurs. The binding constant for PPIX is lower than $TPPS_4$ ($1.67 \pm 0.62 \times 10^5\ M^{-1}$ and $3.11 \pm 0.41 \times 10^5\ M^{-1}$ respectively) while the number of binding sites is the same for both (~ 1). Also, the quenching of tubulin shows a larger Stern-Volmer constant for $TPPS_4$ than PPIX which may indicate a different location of the binding sites. Circular dichroism of both porphyrins also showed that there is no distortion of the porphyrin macrocycle upon binding.

We also investigated the effect of the porphyrins on tubulin polymerization using turbidity assay. Polymerization studies were carried out at a 1:1 ratio of tubulin:porphyrin(~10μM) and showed that in modified PIPES buffer at 37°C the polymerization of tubulin proceeds very slowly except in the presence of a reagent such as paclitaxel. These studies revealed that polymerization of tubulin occurred more slowly, increasing the nucleation phase and growth phase of microtubules. Simulation of potential porphyrin binding sites using ArgusLab showed that $TPPS_4$ and PPIX have affinity to sites that do not overlap other anti-microtubule ligands such as paclitaxel, colchicine, and vinblastine.

Table of Contents

Abstract **1**
Acknowledgements **3**
Chapter 1: Introduction: **4**
Chapter 2: Background: **7**
Hypothesis 15
Project Goal 16
Turbidity assay 16
Chapter 3: Materials and Methods: **20**
Materials 20
Chemicals 20
Buffers 20
PPIX 20
$TPPS_4$ 21
GTP 21
Paclitaxel 21
Colchicine 21
Vinblastine 21
Tubulin 22
Methods 22
Turbidity 22
Tubulin Alone 23
Tubulin & Paclitaxel 23
Tubulin & alkaloids 23
Tubulin & GTP 23
Tubulin & porphyrin 24
Temperature Control 24
Instruments 24
UV absorption spectrophotometer 24
Circular Diochroism 24
Chapter 4: Results: **25**
Flurorescence 25
Docking Simulations 27
Cirular Diochroism 28
Turbidity Assay 28
Chapter 5: Discussion: **33**
Controls 33
Kinetic Analysis 33
Future Directions 38
References **40**
Appendix **41**
A.1 Fluorescence 41
A.2 Docking Simulations 42

My Sincere Gratitude

To my wife to be, Veronica Antonieta Mendez Flores.
I began this project when we fell in love. Now I am closing this chapter and beginning a new one with you.
Te amo, mi Corazon.

To my Mom & Dad for always being there and supporting my endeavors. For always encouraging me to pursue my dreams. To my Brothers and Sister for always challenging me. To my family for making life memorable.

To my mentor Dr. Lorenzo Brancaleon for always pushing me to reach the finish line and for his most unconditional patience. For never holding me back and always ready to take on the next challenge.

---

*To the MARC U*STAR program and all the staff for their support of my research. Dr. Gail Taylor for her teaching and guidance.*

To the Honors College, for effective and great advice. For giving me the opportunity to conduct undergraduate research. To Dr. Ann Eisenberg, for her never-ending support and encouragement.

To the Supplemental Instruction program for allowing me the opportunity to help others. To Maggie and Cyndi for their faithful encouragement.

Last but not least, to my lab group, Steve, Ivan, Sam, Miguel, Nick, Rolando, John, and Kate for making a great research environment and team.

Chapter 1: Introduction:

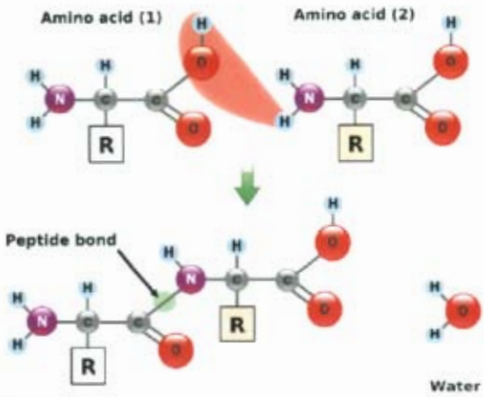


Figure 1 Peptide Bond
This shows the covalent bond produced by the carboxylic acid (COOH) reacting with the amine group (NH_2) to form water and a peptide bond.
http://en.wikipedia.org/wiki/Image:Peptidformationball.svg

Proteins comprise the backbone to cellular structure and function. Made from sequences of amino acids they form long chains by creating peptide bonds*. Amino acids are the natural building blocks of proteins. There are twenty essential amino acids each with an amino group (NH_2), α-carbon, side chain, and carboxyl group (COOH). Each amino acid has a unique functional side chain. The variation in amino acid sequence directs the proteins structure. Four degrees of structure are intrinsic to each protein. The primary structure (1^0) is the sequence of amino acids as mention above. This essentially is the linear order of amino acids. Peptide bonds hold these amino acids together by binding the amino group with the carboxylic group of the subsequent amino acid in a covalent bond(Figure 1). The secondary structure (2^0) is how different regions of the primary structure arrange within a given sequence. The α helix is a basic structure of a linear arrangement that forms by hydrogen bonds between the amino hydrogens and carboxyl oxygens(Figure 2). These are the hydrogen-bond donors and acceptors respectively. The tertiary structure (3^0) is the overall conformation of the protein in 3D space. This is very important because the folding of the protein is crucial to its function. For a macromolecule such as a

* These are bonds that form peptides which are small linear chains of amino acids. Proteins use the same bonding mechanism for its primary structure. Proteins are long chains of amino acids.

microtubule (MT) the functional single subunit is the protein tubulin. The tertiary structure of tubulin is important for its potential to polymerize. The quaternary structure (4^0) is the overall structure of each subunit to form a macromolecule such as a microtubule.

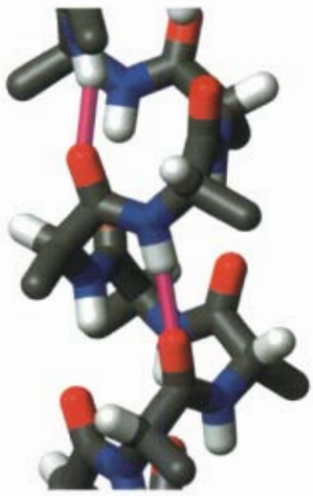


Figure 2 α helix
The hydrogen bonds are shown in pink. They are formed between the carboxyl oxygen (red) and the amino hydrogen(gray)

Tubulin is a globular protein that forms MTs, as mentioned above, which are involved in cell morphology and cell signaling[5]. Nucleotides like guanosine-5'-triphosphate (GTP) bind to the α-tubulin and β-tubulin monomers. However, the β-tubulin has the ability to hydrolyze* GTP to make guanosine 5'-trihydrogen diphosphate (GDP). This mechanism gives the MT dynamic instability and allows it to be flexible in performing its role within the cell. To counteract this dynamic instability the anti-microtubule drug paclitaxel was introduced. This drug binds to the α/β dimer and hyper-stabilizes the MT structure. This prevents the cell from dividing which ultimately leads to cell apoptosis•. The significance of paclitaxel affect on microtubules is the potential for targeting cancer MTs. Research has shown that some porphyrins have similar affects on MTs as well [5, 6].

Porphyrins are heterocyclic macrocycles which come in many varieties and functions. As you can see in Figure 3 the basic meso porphyrin is chlorin. This porphyrin is the basis for the macrocycle of the porphyrins that we studied. Many porphyrins are photosensitizers and some are used in photosynthesis, others are involved

* To break up polymers by reacting with water, in this case β tubulin is able to break off one of the phosphates on GTP to form GDP
• Apoptosis is a form of programmed cell death.

in heme functions of the blood. The importance of the porphyrins that we studied, is that one is hydrophilic and the other hydrophobic.

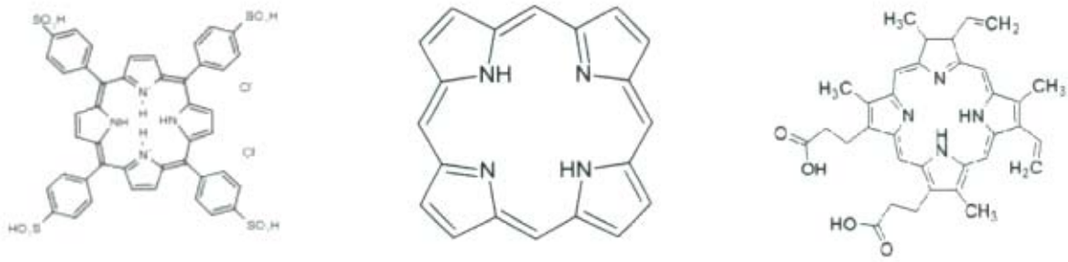


Figure 3 Porphyrins
In the middle is the simplest form of a porphyrin (chlorin) which has the four pyrrole subunits with carbon bridges in between each. Capping each pyrrole is a nitrogen and additional hydrogen bridge. On the left is *meso*-tetra (4-sulfonatophenyl)porphine ($TPPS_4$) and on the right is protoporphyrin IX (PPIX). Both have the simplest macrocylce unit chlorine and different reacting groups. $TPPS_4$ is hydrophilic while PPIX is hydrophobic.

Chapter 2: Background:

Cancer has plagued mankind since the beginning of existence; however with the increase of technology and manufacturing we have also seen a proliferation of cancer related deaths. The reason for the increase in Cancer diagnosis is the increase of carcinogens or radioactive materials that are found in a majority of manufacturing plants. Cancer is the uncontrolled division of cells that invaded other cell tissues. Treatments have been developed such as chemotherapy or radiation that prolong life expectancy and in some isolated cases provide a cure. The bulk of research has been directed toward finding a cure for different types of cancer but palliation is just as important. In 1958 the National Cancer Institute commissioned botanists from the Department of Agriculture to collect over 30,000 plant samples for anticancer research. Included in these samples were twigs, needles, and bark from *Taxus brevifolia* or more commonly known as the Pacific yew tree collected by Arthur S. Barclay. Then, in 1963 Monroe E. Wall and Mansukh C. Wani at the Research Triangle Park discovered that Pacific yew had anticancer properties in rodent tumors. Several years later they isolated the compound paclitaxel and modeled its structure[7].

From their discovery Susan B. Horowitz at Albert Einstein College of Medicine in New York solved the mystery of how paclitaxel works. This discovery has proven very important in the battle against cancer. However, when paclitaxel was first discovered the process involved harvesting the compound was very inefficient and detrimental to the environment. The accumulation of one gram of paclitaxel required the bark of one 40 ft Pacific yew which, to say the least, was around 200 years old. The

source of Pacific yew was also scarce because they are one of the slowest growing trees. Another disadvantage, as with all forms of chemotherapy, for the drug paclitaxel is limited to the amount each patient can endure.

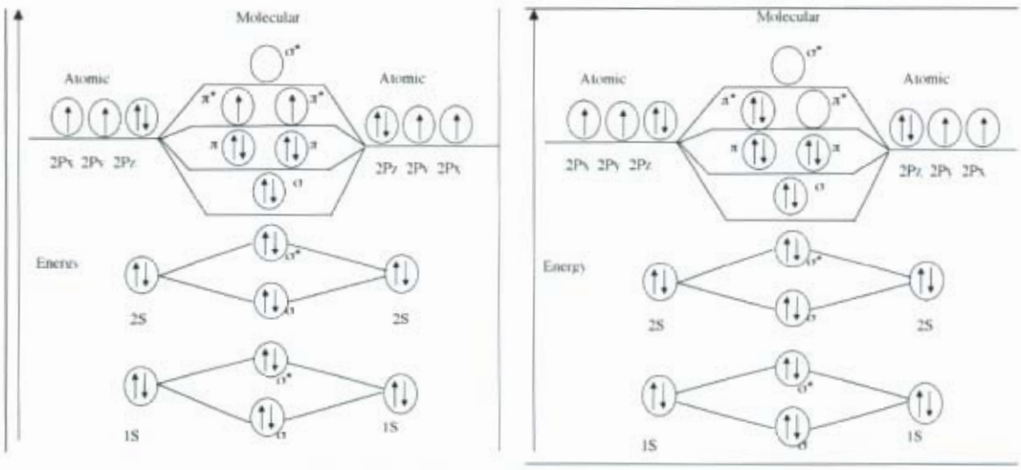


Figure 4 Molecular orbital (MO) arrangement of triplet oxygen (left) and singlet oxygen (right) [1]

These limitations lead researchers to find safer alternatives to cancer treatment such as photodynamic therapy (PDT). PDT involves the use of a photosensitizer, light, and tissue oxygen. A photosensitizer is a chemical compound that is excited by light of a particular wavelength. In this field scientists are concerned with porphyrin photosensitizers. The light used in these procedures is usually in the visible or near infrared spectrum. The photosensitizer (usually a dye) is first excited from a ground singlet state to an excited singlet state. The excited photosensitizer has typically a high quantum yield for the formation of a triplet excited state[*]. Because the transition back to the ground (singlet) state is forbidden by transition selection rules ($\Delta S = 0$) a molecule can occupy the singlet state for a relatively long time (on molecular scale) ranging from

[*] where the electron has "flipped" its original spin

μs up to seconds. In this time the excited molecules can exchange energy with a diffusing oxygen molecule (O_2) which is also a triplet in its ground state (Figure 4).

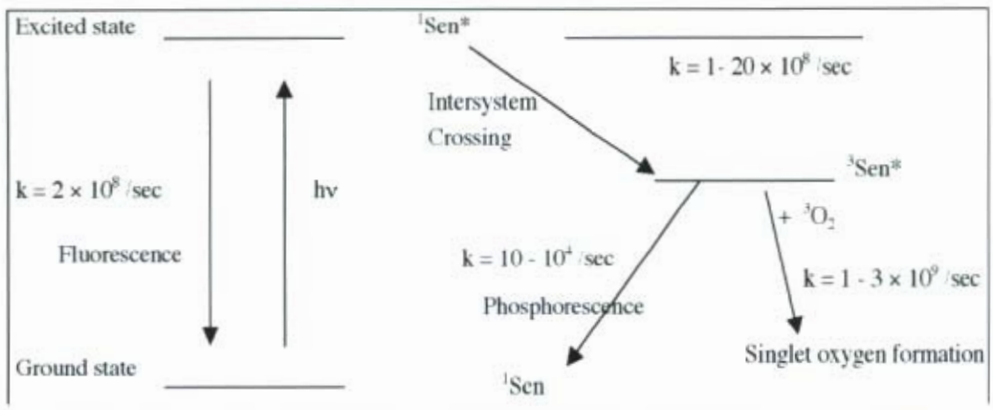


Figure 5: The chemical mechanism for the formation of singlet oxygen in the presence of sensitizer, light and triplet oxygen showing the excitation and deactivation of photosensitizer in the formation of singlet oxygen [1].

The energy transfer between the two triplets now produces an allowed transition ($\Delta S = 0$ or $\Delta L = \pm 1$) when the two triplets transition to singlets. The excited molecule returns to the ground (singlet) state and molecular oxygen is excited to its singlet state (Figure 5).

Singlet oxygen is a highly reactive state that readily interacts with surrounding molecules. In cells, the presence of singlet oxygen is extremely toxic and can lead to cell death if the concentration of singlet oxygen is large enough. Cell death normally occurs in traumatic ways (necrosis) [8] However, under controlled condition of photosensitizers and irradiation it has been shown that apoptosis can be promoted[8]..Roeders and coworkers (1994) showed that O_2 development in erythrocyte ghosts* was demonstrated by its light emission at 1270nm. In summary, photosensitizers upon irradiation with UV, visible and sometimes near-IR radiation (at 1270 nm the difference between the ground

* The membrane and cytoskeleton elements of a red blood cell without cytoplasmic contents, but with a maintained original morphology.

state and excited state is 94.2 KJ [9]) get promoted to the first excited singlet state from which they decay, through intersystem crossing (ISC), to their lowest excited triplet state (Figure 6).

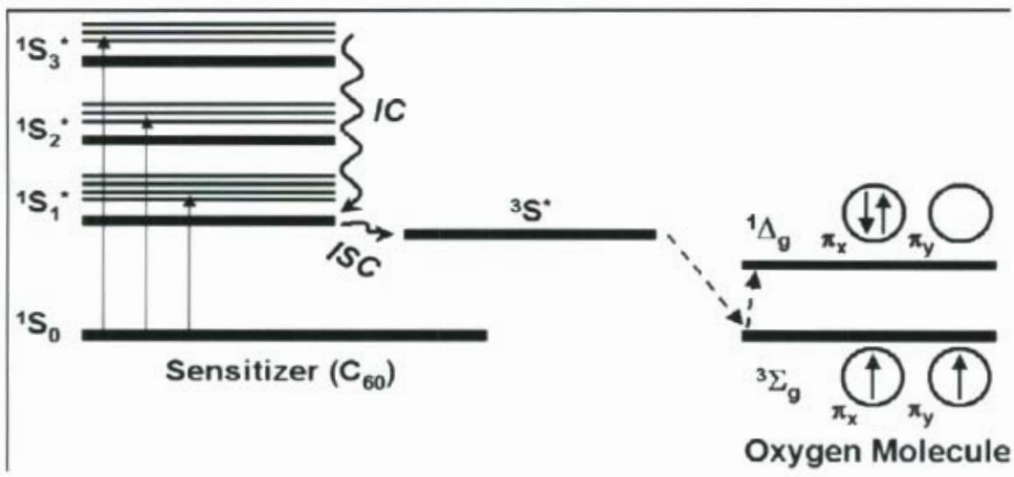


Figure 6: Jablonski diagram showing the generation of singlet oxygen through a photoreaction mechanism. The sensitizer is first excited using UV or near IR light then through internal conversion(IC) comes to back to S_1 state which deactivates through inter system crossing (ISC) to its triplet state. This triplet state then reacts with an oxygen molecule through energy transfer, thus promoting the oxygen molecule to a singlet state[3].

As mentioned before, singlet oxygen is very reactive and in cells can damage basically every vital molecular component (DNA, proteins, phospholipids (membranes), etc.). The first trials of PDT were performed by German physician Friedrich Meyer-Betz on himself in 1913. PDT was not widely known until several decades later when Thomas Dougherty founded the International Photodynamic Association. Because of Dougherty's contribution in 1986, PDT has become a valuable tool to surgeons by increasing the probability of a turning an inoperable cancer locus to an operable one[8].

PDT, as described above, however has several limitations including (i) the oxygen dependence of the process (no oxygen → no-singlet oxygen → no damage → no cell death) and (ii) the apparent lack of specificity for the damage as molecular oxygen would

react with every molecule within 100 nm of the point where it is generated. Moreover the above description only tells part of the story. In fact photosensitizer can also produce photodamage through other more local mechanisms such as the formation of radicals[10, 11] or the direct photochemical reaction with neighboring molecules (charge transfer, isomerization, etc.). These mechanisms may or may not be oxygen dependent, thus the focus of our research is more correctly on phototherapy rather than PDT where the "dynamic" factor due to diffusing molecular oxygen, is not necessarily involved in the damage. Because this is a more local effect it can be expected to be more specific too and that is the reason why we focused our attention to the interaction of certain photosensitizers with certain proteins, which have been suggested to represent possible targets *in vivo*.

Over fifteen years ago it was discovered that some porphyrins (in particular *meso*-tetra (4-sulfonatophenyl)porphine ($TPPS_4$) and meso-tetrametyl-pyridyl porphyrin (TMPP) prevented the formation of microtubules [12] (see below). In vivo, microtubules are formed by the organized, reversible assembly of tubulin hetero (α,β) dimers [13] (Figure 4).

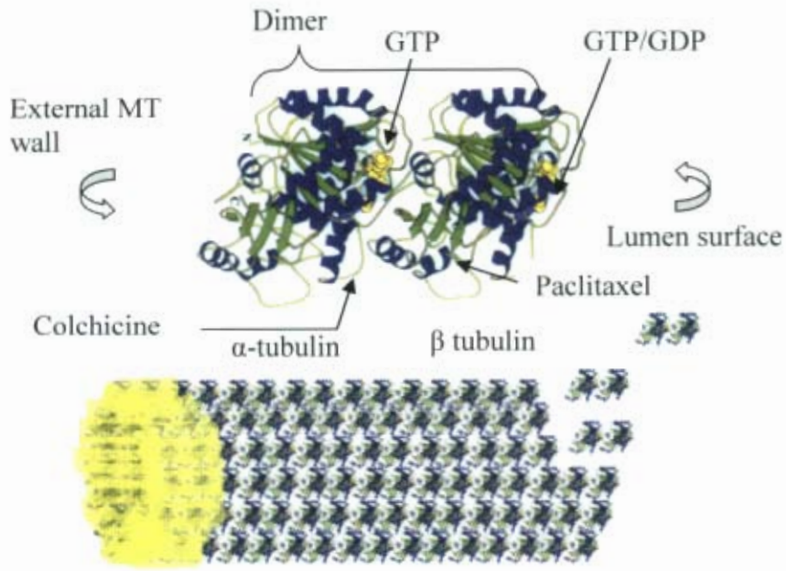


Figure 7: Representation of the αβ tubulin heterodimer(top). The sites where GTP and GDP bind have distinct locations. Only on the β tubulin can GTP hydrolyze to form GDP. Colchicines, which inhibit polymerization, bind to the GTP site not allowing the heterodimers to form microtubules. Microtubule (bottom) formation of 14 dimers in a rod like tubular structure (yellow)[2].

Microtubules are involved in many functions including cell mitosis, cell signaling and cellular morphology[14]. Tubulin heterodimers contain several functional components or domains. One domain binds to guanosine-5'-triphosphate (GTP). GTP binds both forms of tubulin, however while in α-tubulin it remains at the α/β interface, in β-tubulin GTP is hydrolyzed to GDP and this step is fundamental to control the reversible polymerization of microtubules *in vivo*. Essentially the GTP which is attached to β monomer must retain its conformation and is responsible for the microtubule elongation and structure.

GDP, which is first located on the β monomer as GTP then transformed through hydrolysis, is crucial to disassembling the microtubule structure (Figure 7). Another site, located in the portion of β -tubulin that faces the lumen of the microtubule, binds to taxoid drugs (Figure 8). A tubulin dimer provides a binding site for colchicinoids at the

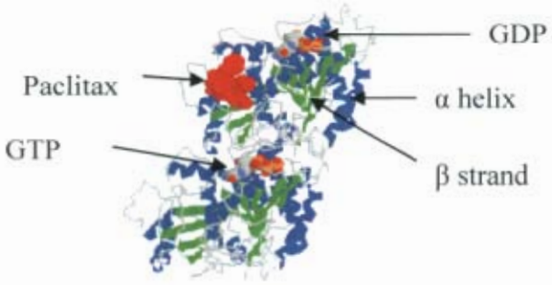


Figure 8: This is a protein database file showing the tertiary structure of α/β tubulin dimer. α tubulin is located on the bottom and β tubulin is located on the top. The α helices are indicated as blue and the β strands are indicated as green. The GTP and GDP nucleotides are denoted in CPK colors and Paclitaxel is in red.

α/β interface but distinct from the GTP site (Figure 9). At the same interface there is a shared (between β and α) site for so called vinca-alkaloids (Figure 9). A number of docking sites for proteins (e.g. kinesin) have also been shown. The microtubule structure consists of tubulin monomers that form a repetitive circular pattern arrangement as a long tube or protofilament. The cylindrical pattern is on the basis of a parallel formation of tubulin monomers[14]. Each tubulin structure consists of a core of β sheets and surrounding helices. The N terminal half forms a Rossman fold, which is an open α/β structure[14, 15] (Figure 10). This fold is comprised of six parallel β strands and three surrounding helices. This is then circumscribed by two antiparallel helices.

Paclitaxel (Taxol), when bound to microtubules, arrests the hydrolysis of GTP. This is accomplished by inhibiting the GTPase reaction by tubulin itself. It slows down the dissociation rate constant of tubulin from MTs[6]. Thus GTP can only hydrolyze on β and not α tubulin. The probability that paclitaxel will bind to β tubulin is dependent on the residues surrounding the binding pocket[16]. Certain cancers contain isotypes of β tubulin that are not affected by paclitaxel presence.

When paclitaxel binds properly it promotes stabilization by inhibiting the GDP instability. Thus the microtubules that form are not able to carry out their role due to

their lack of dynamic instability. Stabilization of microtubule, as literature suggests, results in apoptosis of cancer cells by promoting binding to death receptors designed for programmed cell death [17]. As mentioned before, porphyrins were used in photodynamic therapy to damage and shrink cancer cells. It has been reported that $TPPS_4$ shows similar cellular effects with stabilization of microtubules [18]. Thus it appears that porphyrins such as $TPPS_4$ can lead to apoptosis of cancer cells with a mechanism similar to paclitaxel. It is thus important to establish whether porphyrins compete with paclitaxel for the same binding site of tubulin or if the same stabilization effects could be achieved by binding tubulin at separate sites.

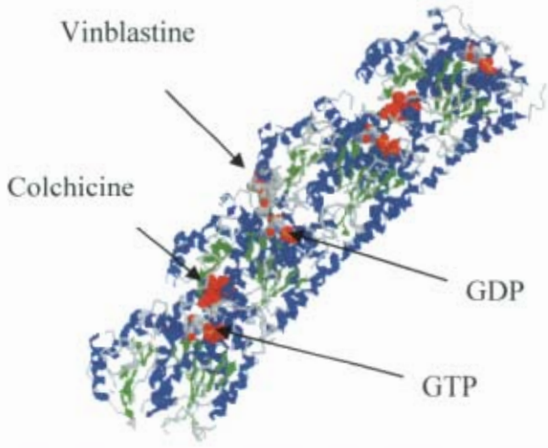


Figure 9: This is a protein database file of two α/β dimers. The alkaloids colchicine and Vinblastine bind to tubulin inhibiting polymerization. Colchicine binds from (left to right) between the α/β interfaces. Vinblastine binds to the β/α interface but is extended out. Thus Vinblastine inhibits polymerization at low concentrations but forms paracrystals at higher concentrations[4].

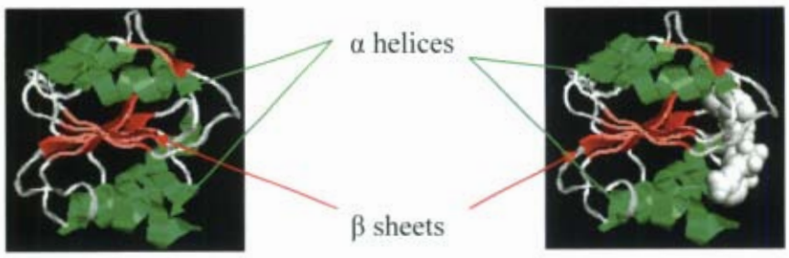


Figure 10: The Rossman fold (left) is a common motif for proteins that bind with nucleotides (right) as shown in white. The Rossman fold consists of an open α/β structure.

One hypothesis is that if similar results are evident then polymerization of bound tubulin should be the same for both paclitaxel and $TPPS_4$. Thus $TPPS_4$ should promote polymerization as well. This point is debatable since it has been shown that $TPPS_4$, *in vitro*, inhibits polymerization in a mechanism similar to colchicines[5]. Our research proposal is thus made even more intriguing by the possibility that $TPPS_4$-mediated stabilization of microtubule is a light-dependent effect instead of being driven solely by binding as is the case for paclitaxel. Previous work from our group showed the binding of tubulin to porphyrins. Both PPIX and $TPPS_4$ appear to bind tubulin as probed by the shift of the fluorescence maximum of both porphyrins[19] (Figure 11).

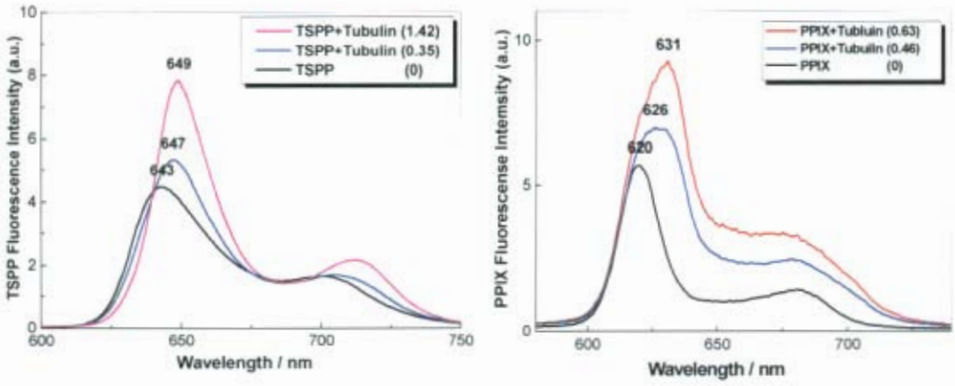


Figure 11: fluorescence emission peak blue shifts of $TPPS_4$ (left) and PPIX (right) upon addition of tubulin of $TPPS_4$ and PPIX (the numbers in the brackets are tubulin/porphyrin molar ratio)

Our preliminary data shows that $TPPS_4$ and PPIX bind tubulin with the same stoichiometry (1:1) however, the binding constant of $TPPS_4$ was higher than PPIX (K_b = $3.11 \pm 0.41 \times 10^5\ M^{-1}$ vs. $1.67 \pm 0.62 \times 10^5\ M^{-1}$ respectively). Moreover, the porphyrin-induced quenching of the intrinsic tubulin fluorescence showed that $TPPS_4$ quenched tubulin at a rate nearly double the one of PPIX. Thus our data showed that it was possible for PPIX and $TPPS_4$ to bind to separate sites. This project focused on determining possible locations for the binding site of PPIX and $TPPS_4$, as well as establishing whether one (or both) porphyrin(s) affect MT polymerization in comparison with other anti-microtubule ligands.

Turbidity assay (scattering)

The kinetics involved in microtubule assembly is an important parameter to consider. The rate of a reaction is defined as the change in concentration of reactants or products over time. We now consider freely distributed monomers that go through two stages of polymerization. The first stage is the nucleation process, when the first thermodynamically unstable nucleus of polymerization forms. The second stage is post nucleation in which monomers add to form polymers of ranging degrees in solution [20]. An equation for the simulation of kinetics involved in microtubule formation was formulated by Hall *et. al.* and is described by [20, 21] Eq. (1).

$$P_i + M \underset{k_{i-}}{\overset{k_{i+}}{\rightleftarrows}} P_{i+1}. \qquad \text{Eq. (1)}$$

Where P_i denotes the polymer of degree i and M denotes the concentration of free monomer. These formulations were on the basis of a few assumptions. First assumption was that the forward and reverse rate constants were considered equivalent prior to

nucleation. Secondly a similar consideration was made for the growth steps after nucleation. These rate constants were denoted as

$$k_{N+}\ ,\ k_{N-}\ ,\ k_{G+}\ ,\ k_{G-}$$

where N is the stage prior to nucleation and G is the growth stage post nucleation. Also, positive denotes the forward step and negative is the reverse step. When dealing with growth we consider these as the association and dissociation constants. A set of interrelated first-order differential equations (ODE) was also solved by Hall *et. al*[20, 21]. which denotes the rate of change of the concentration of species of degree *i*. This initial rate was denoted by Eq.(2)

$$d(P_i)/dt = -k_{i+}(P_i)(M) - k_{i-}(P_i) + k_{i+}(P_{i-1})(M) + k_{i-}(P_{i+1}). \qquad \text{Eq. (2)}$$

$$d[N_i]/dt = -k_{G+}[N_i][M] - k_{N-}[N_i] + k_{N+}[N_{i-1}][M] + k_{G-}[P_1] \qquad \text{Eq. (3)}$$

$$d[P_Z]/dt = -k_{G-}[P_Z] + k_{G+}[P_{:-1}][M]$$

Then was solved previously in [20] and determined to be Eq. (3) where N denotes the nucleation step and P denotes the polymer of ranging degrees.

The distribution of microtubules in solution can be transformed to apparent absorption. An important fundament of UV-absorption spectroscopy is that each functional group within a molecule has its own absorption band[22, 23]. Certain types of transitions of molecules are rotational, vibrational, and electronic (outer and inner shell).

Electronic transitions are initiated by absorbing light at a specific wavelength which ranges from visible to UV light. When molecules absorb light they transition from a lower energy state to a higher energy state. This technique can be used to monitor concentration and conformational changes in biological molecules[22, 23].

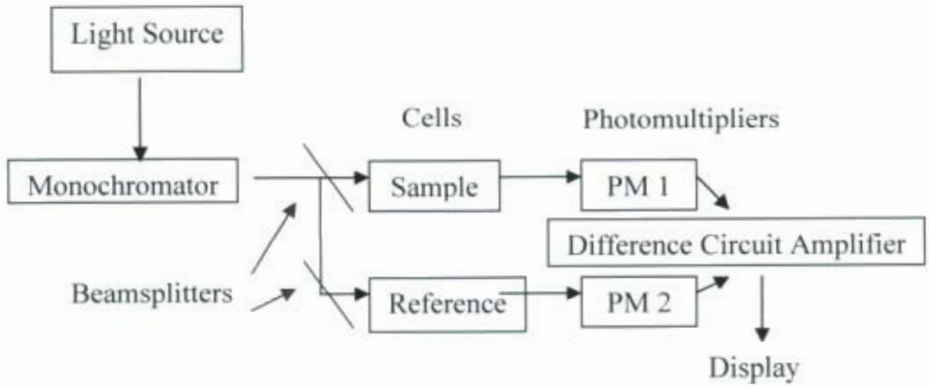


Figure 7: The general setup of electronic absorption intstrument. The monochromator is used to disperse the light into various wavelengths. A beamsplitter is used so that the intensity of the sample (I) and also the initial intensity (I_o) of Beer's Law can be recorded simultaneously. The compartments hold the sample and references cells. Then the light is passed to a photomultiplier to increase the signal so that a display can be created by a diffence circuit.

The general setup of a recording spectrograph consists of a light source, monochromator, beamsplitter, cell compartments, photomultiplier tubes (PMT), and a difference circuit amplifier as shown in Figure 7. In this procedure however, we will not be recording absorption. The apparent absorption is due to the turbidity of the solution. Thus light is not being absorbed by the molecule but it is being scattered.

Turbidity was further re-examined by Hall *et. al.* who produced a model for the turbidity signal τ which included a scattering exponent that could be retrieved from a slope of the linear regression of $\ln \tau$ against $\ln \lambda$ which is written as Eq. (4)

$$n(t) = \frac{\mathrm{d} \ln \tau(t)}{\mathrm{d} \ln \lambda} \qquad \text{Eq. (4)}$$

This is equal to the theoretical approach by Hall *et. al.* and is given by

$$= -4 + \mathrm{d} \ln \Psi / \mathrm{d} \ln \lambda + \mathrm{d} \ln J(t) / \mathrm{d} \ln \lambda. \qquad \text{Eq. (5)}$$

where

$$\psi(\lambda) = \{n_o(\lambda)\}^2 \left(\frac{\mathrm{d}n}{\mathrm{d}c}(\lambda) \right)^2 \qquad \text{Eq. (6)}$$

and

$$J(\{c\}, \lambda) = \sum_i M_i c_i Q_i(\lambda). \qquad \text{Eq. (7)}$$

where ψ denotes the wave equation as a function of the solvent refractive index and the specific refractive increment. J denotes the summation of the product of the molecular weight, weight/volume concentration, and the transmittance particle dissociation factor. The dependence of the turbidity signal on ψ can be eliminated by multiplying by a normalization factor F which is $1/\psi$. Thus Eq. (7) provides a direct connection between the distribution of oligomeric species which is given by J and the wavelength exponent n. M_i denotes the molecular weight, c_i is the weight/volume concentration, and Q_i is the transmittance particle dissipation factor which was previously determined by Hall *et. al.* [20, 21].

Chapter 3: Materials and Methods:

Materials:

Chemicals:

Tubulin (>99% pure) was purchased from Cytoskeleton Inc. (Denver, CO). $TPPS_4$ was purchased from Frontier Scientific (Salt Lake, UT) while PPIX and spectroscopic grade dimethyl sulfoxide (DMSO) were purchased from Sigma-Aldrich (St. Louis, MO). All products were used without further purification.

Buffers:

Deionized water was used to prepare aqueous buffers according to Cytoskeleton. This buffer is a mixture of 80mM PIPES, .5mM EGTA, 2mM $MgCl_2$, and 5% glycerol. All reagents were purchased from Sigma-Aldrich. NaOH was added to raise the pH level from pH 3. All experiments were conducted at pH 6.6.

Sample Preparation:

PPIX:

PPIX was dissolved in buffer and compared to the absorption of PPIX in dimethyl sulfide oxide (DMSO). Using absorption spectroscopy the concentration of the PPIX stock was adjusted to 200 μM assuming the optical density of PPIX in DMSO at 405 nm is $\varepsilon = 2.42 \times 10^5\ M^{-1}\ cm^{-1}$[19, 24]. The absorbance of our PPIX in buffer was approximately .2 a.u. which was equivalent to 10μM in DMSO. This solution was used as the stock for our experiments. The addition of 25μl of PPIX stock in 500μl of tubulin solution produced 10 μM concentration of both.

$TPPS_4$:

This porphyrin being very hydrophilic was diluted directly into buffer. Using absorption spectroscopy and assuming that its optical density at 413nm is $\varepsilon = 5.1 \times 10^5\ M^{-1}\ cm^{-1}$ [19] the concentration was adjusted to 200 μM. This solution was used as the stock for our experiments. The addition of 25μl of $TPPS_4$ stock in 500μl of tubulin solution produced 10 μM concentration of both.

GTP:

This nucleotide was dissolved directly into buffer. Using a molar extinction coefficient of $\varepsilon = 13.7 \times 10^3\ M^{-1}\ cm^{-1}$ at 253nm (Sigma), a stock of 200 μM was prepared. An aliquot of 25 μl was then added to make a 10μM solution in 500 μl of tubulin.

Paclitaxel:

Paclitaxel with a molecular weight of 853.92 g/mol was prepared by weighing 1mg and dissolved in DMSO. Then the initial stock was diluted in buffer to yield a 10μM concentration and thus keeping the concentration of DMSO in aqueous solutions < 1%.

Colchicine:

Colchicine was dissolved in buffer and the concentration was adjusted to 200μM assuming the optical density at 350nm is $\varepsilon = 16.6 \times 10^3\ M^{-1}\ cm^{-1}$ [25]. The addition of 25μl in 500μl tubulin yielded a 10μM concentration of both.

Vinblastine:

Vinblastine was dissolved in buffer and the concentration was adjusted to 200μM assuming the optical density at 270nm is $\varepsilon = 14 \times 10^3\ M^{-1}\ cm^{-1}$ (Sigma-Aldrich). The addition of 25μl in 500μl tubulin yielded a 10μM concentration of both.

Tubulin:

Tubulin was prepared directly in buffer to yield a 10 μM solution. 1mg vials of tubulin were dissolved in 1ml and then split into two vials of 500ul each. One vial was kept for tubulin alone and the other was used to incubate the ligand and tubulin for 30mins at 4^0C The concentration was determined using absorption spectroscopy at 280nm since the molar extinction coefficient of Tubulin at 280 nm is $\varepsilon = 1.15 \times 10^5\ M^{-1}\ cm^{-1}$[19]. The molar ratios of tubulin to ligands was 1:1. The cuvettes were polystyrene UV-visible and purchased from Fisher Scientific. The cuvettes were semi-micro 4mm, however oriented so our pathlength was 1cm.

Methods:

Turbidity:

Prior to each polymerization recording, the absorbance of the sample was scanned from 250nm to 450nm. After the polymerization was recorded the absorbance was scanned again. All turbidity experiments were carried out using a tubulin concentration of 10μM with or without ligand at 37^0 C. First the tubuling 1mg/ml vials were split into two vials of 500μl each. One vial of tubulin had the addition of a ligand. The ligand and tubulin solutions were first incubated for 30min at 4^0 C before being recorded for an hour at 340nm in a semi-micro cuvette. The cuvette was orientated so the optical path length was 1cm and the window was 4mm. This was followed by the recording of tubulin alone, which was our control. The recordings were performed with measurements taken every 30s and an integral time of 3s. Recordings of tubulin polymerization under different conditions were taken.

Tubulin Alone:

Turbidity from solutions containing only tubulin were used as a baseline controls. It was observed that the rate of polymerization of tubulin was very slow without the presence of paclitaxel or GTP.

Tubulin & Paclitaxel:

Another control was obtained by adding to the tubulin solution an aliquot of paclitaxel in DMSO so that the final concentration of paclitaxel is 10 μM. The rate of polymerization was recorded. Even at room temperature, paclitaxel induces polymerization of tubulin [26].

Tubulin & alkaloids:

The experiment described for paclitaxel was repeated using vinblastine and colchicine at the same 10 μM final concentration. Both vinblastine and colchicine inhibit tubulin polymerization at higher concentrations than the critical concentration of tubulin[5]. They both were used as a reference for the effects of porphyrins on microtubule polymerization

Tubulin & GTP:

GTP is the "natural" ligand of tubulin and induces polymerization of tubulin *in vitro* and *in vivo*. GTP at a final concentration of 10 μM was added to the tubulin solution and the rate of polymerization was measured and used as a reference.

The experiments above form the baseline against which we compared the binding of tubulin. The effects of the above ligands as well as their location on tubulin are well characterized, thus to investigate the location of the binding site for $TPPS_4$ and PPIX we

looked at the effect on polymerization of the competition of each porphyrin with each ligand.

Tubulin & porphyrin:

Polymerization was investigated upon addition of each porphyrin, to a final concentration 10 μM, to the solution containing tubulin. This allowed us to investigate any polymerization that may be induced by porphyrins themselves.

Temperature Control:

The experiments described above were carried out at 37^0 C by using a peltier temperature control unit (Thermo Electron). The reason for this condition is that polymerization of tubulin is strongly temperature dependent and obviously the most important temperature to investigate is the physiological one ($37\ ^0$C). At this temperature the kinetics of polymerization are much faster thus recordings spanned for approximately one hour with recordings done every 30s.

Instruments:

UV absorption spectrophotometer:

This instrument is a Nicolet Evolution 300 series Thermo Electron manufactured UV-absorption spectrometer. Refer to Figure 7 for a schematic of the essential components of this instrument.

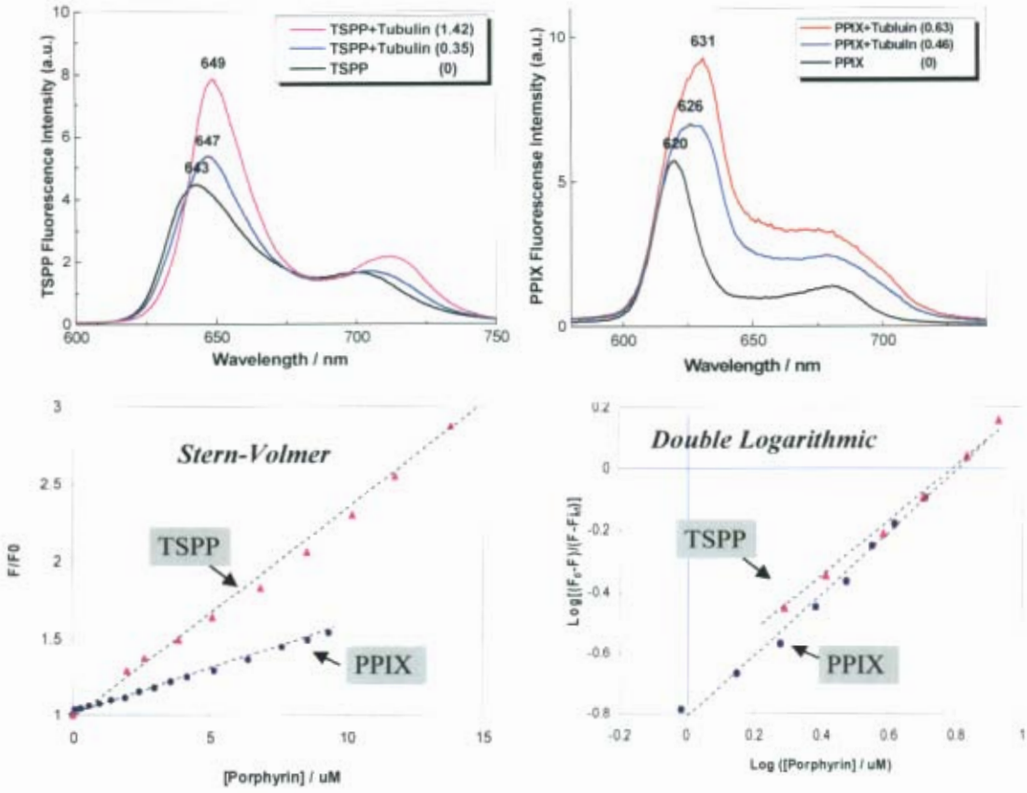
Circular Dichroism:

This measurement was recorded using a Jasco J-815 spectrophotometer. Scans were recorded at 20nm/min at a resolution of 1 nm. These scans were averaged over 3 runs.

Chapter 4: Results:

Fluorescence of $TPPS_4$ and PPIX bound to tubulin:

The fluorescence emission of $TPPS_4$ and PPIX previously done by our research group (as seen in Figure 12) shows that upon the addition of tubulin at different molar ratios there is an increase in intensity and red shift of the emission peaks from 643nm to 649nm and 620nm to 631nm respectively. Stern Volmer analysis is used to understand the Photophysical deactivation process. The intermolecular deactivation is the increase in decay rate of a chemical in an excited state by the presence of another chemical. Our Stern-Volmer analysis reveals that $TPPS_4$ has a faster quenching rate than PPIX. The ouble logarithmic plot shows that tubulin has a binding site for both (~1).



	K_s / $^{5}M^{-1}$	n	K_d / $^{-6}$ M
TSPP	**1.7 ±**	**0.81 ± 0.10**	**4.9 ± 1.2**
PPIX	**0.54 ± 0.03**	**0.85 ± 0.06**	**6.0 ± 1.2**

*K_s: static quenching constant; n: binding sites; $_d$: dissociate

Figure 12: (top) This is the fluorescence emission peaks of TSPP and PPIX upon the addition of tubulin. Notice the increase in intensity and red shifts demonstrating that binding is occurring. (bottom) Static quenching of tubulin fluorescence upon addition of TSPP and PPIX. The Stern-Volmer shows that TSPP has a larger rate for quenching. The double logarithmic plot indicates that they both have a binding site (~1).

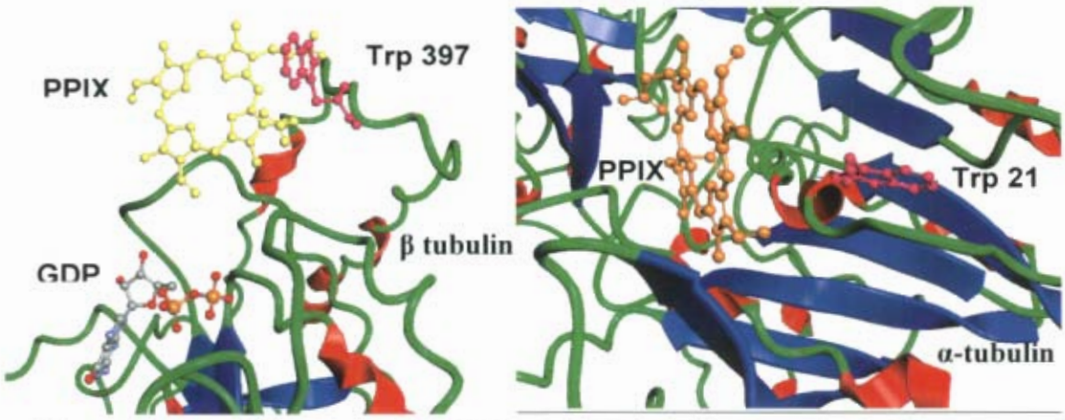
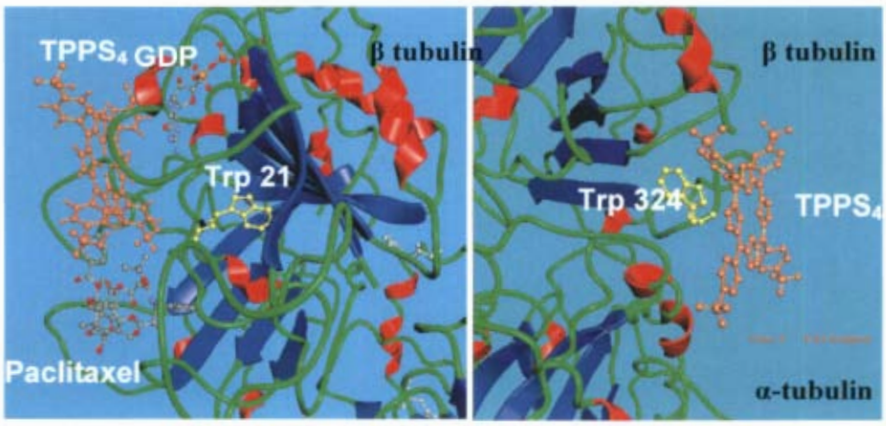


Figure 6:
PPIX: Yellow
Trp: Violet
GDP: CPK

These are simulations of PPIX binding to a tubulin dimer. PPIX has a binding energy of -11.2 kcal/mol when docked to Trp 397 located on β tubulin (left). PPIX has a binding energy of -10.5 kcal/mol when docked to Trp 21 located on α-tubulin (right).



TSPP: Orange
Trp: Yellow
GDP: CPK
Paclitaxel: CPK

These are simulations of $TPPS_4$ binding to a tubulin dimer. $TPPS_4$ has a binding energy of -10.1 kcal/mol when docked to 21 Trp located on β tubulin (left). $TPPS_4$ has a binding energy of -6.83 kcal/mol when docked to 324 Trp located on β tubulin (right).

Figure 13: **The docking simulations of porphyrins to tubulin using ArgusLab 4.0.1**

Docking Simulations:

Using a molecular modeling and drug docking software called Arguslab 4.0.1 docking simulations were performed (Figure 13) and revealed that $TPPS_4$ and PPIX bind

to two sites with the lowest energy required. (1) $TPPS_4$ may bind to the region close to the paclitaxel, GDP, and Trp 21 located on β-tubulin. (2) This porphyrin also has the possibility of binding to the Trp 324 located on the β-tubulin in the region of the α/β-tubulin interface. (1) However, PPIX has a lowest energy for binding at the Trp 21 on the α-tubulin (just beneath the α/β interface). (2) This porphyrin also has the potential of binding near Trp-397 on the β-tubulin. Table 1 shows the binding energies for the two lowest energy requirements for each site of the porphyrin/tubulin binding.

Docking Site	**(1)**	**(2)**
PPIX	-11.2 kcal/mol	-10.5 kcal/mol
$TPPS_4$	-10.1 kcal/mol	-6.83 kcal/mol

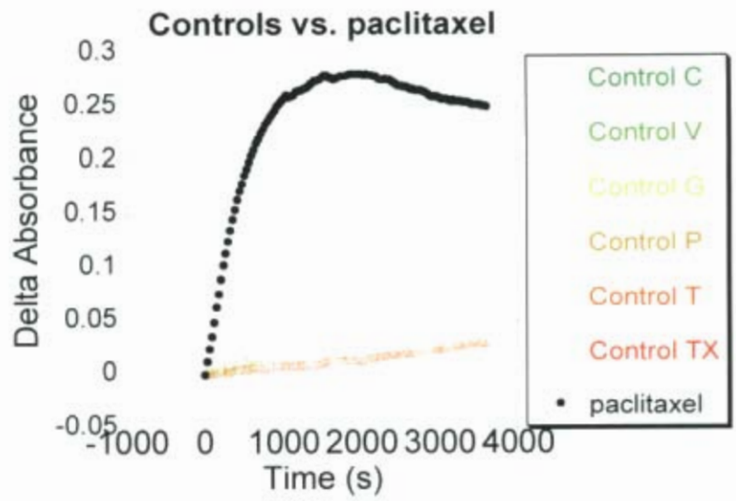
Table 1 Binding energies for $TPPS_4$ and PPIX
These are the lowest binding simulation energies obtained using ArgusLab 4.0.1.

Circular Dichroism:

The results showed no signal in the Soret band for both $TPPS_4$ and PPIX and pH 7. Thus the macrocycle (refer to the Introduction), as seen in Figure 13, is assumed to be planar for both porphyrins upon the binding to the protein. This leads to superficial binding of the porphyrins because there is no distortion of its macrocycle to fit in between the tubulin monomers. The binding of both porphyrins to the protein was verified using fluorescence spectroscopy as mentioned in the Methods section.

Turbidity Assay:

The results of these rates performed, as mentioned above, show that tubulin alone polymerizes very slowly at 37^0 C without the presence of GTP. The rates of these controls, which as mentioned previously, were taken after each run with tubulin and the aforementioned ligand. There were a total of six controls, one for each ligand including



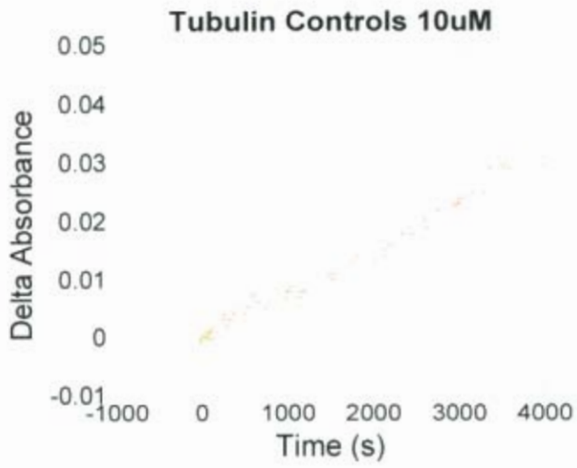


Figure 14: Controls:
These were the controls that were run after each sample with tubulin and ligand. The legend shows the controls along with C, V, G, P, T, and TX denoting colchicine, vinblastine, GTP, PPIX, $TPPS_4$ and paclitaxel respectively. This is not to say that these runs had any ligand in addition. This is only tubulin alone, done after the corresponding sample ligand was run on that day. (bottom) Shows the controls and (top) shows with the rate of tubulin polymerization induced by paclitaxel. Notice that the rates seem fairly similar and consistent in comparison with paclitaxel and tubulin.

paclitaxel, GTP, colchicine, vinblastine, $TPPS_4$, and PPIX which can be seen in Figure 14. Each control was recorded under the same condition except for paclitaxel control which had < 1% DMSO. The rates show that the controls were very similar, however there are some inconsistencies. When plotted in the background of tubulin with paclitaxel, it was observed that the controls showed little or no polymerization.

The rates of both inhibitors colchicine and vinblastine showed no polymerization or turbidity signal as expected[4, 5]. Looking at Figure 15 you will observe that both colchicine and vinblastine showed no signal of turbidity or less than that of tubulin alone.

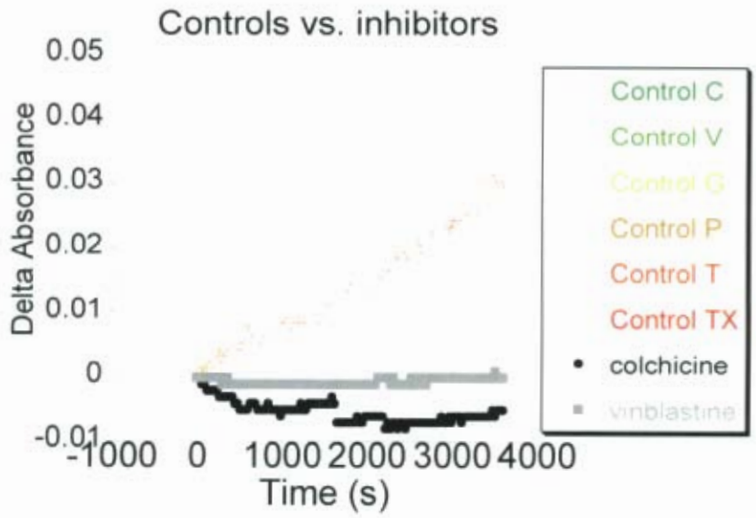


Figure 15: Inhibitors:
These are the rates of both colchicine and vinblastine. Both inhibitors showed no turbidity signal or that less than the rates of tubulin alone as you can see above. Both inhibitors were incubated with tubulin for 30mins at 4^0 C prior to each recording as stated in the methods section

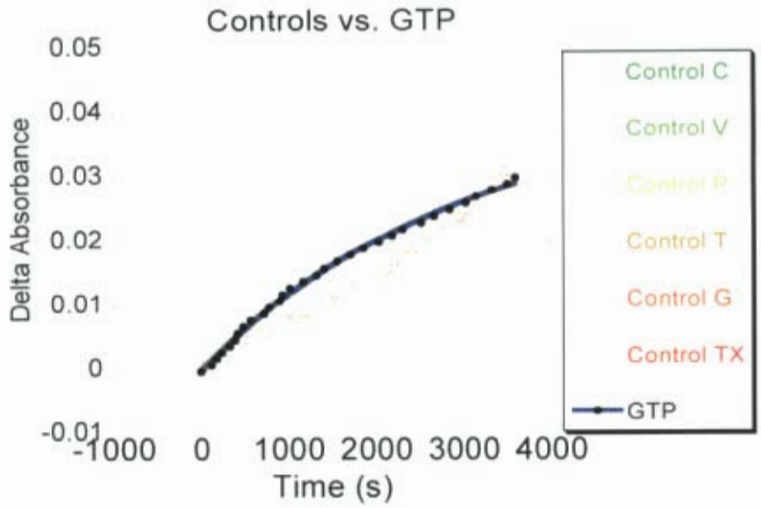


Figure 16: GTP:
This is the rate of tubulin polymerization induced by the nucleotide GTP at 10μM. Notice that GTP sample rate is fairly larger than all of the controls except for one (Control V).

GTP showed a relatively low rate of polymerization at 10μM concentration. As compared with the controls, GTP is larger than the average of their rates (Figure 16).

The assay of both porphyrins showed a slight rate followed by an immediate plateau in signal (Figure 17). In comparison with the controls, both porphyrins seem to show some polymerization of tubulin.

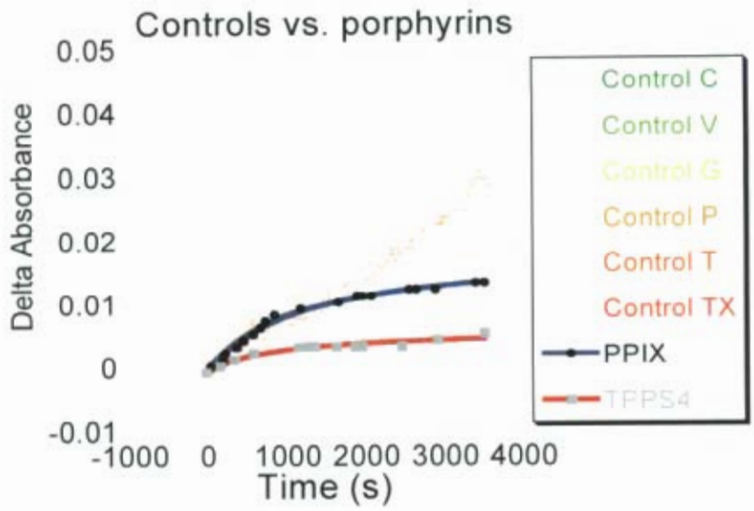


Figure 17: Porphyrins:
These rates have an initial increase in turbidity signal, yet plateau relatively quickly within the first 20min of the measurement. The rates of both porphyrins are unlike those of tubulin alone in that they plateau within an hour of measurement. It is interesting to notice that PPIX has a higher rate than the $TPPS_4$. Remember that PPIX is hydrophobic and $TPPS_4$ is hydrophilic.

Chapter 5: Discussion:

Controls:

The differences in rates of tubulin alone can be explained from the tubulin 1mg/ml which upon splitting into two solutions of 500µl, may have made the final solution ~10µM ± 2µM. This can be seen from the absorbance spectra taken before each rate measurement. The absorbance of tubulin alone at 280nm was 1.5 ± 2 a.u.

Kinetic Analysis

Kinetic analysis was performed by fitting a general one step polymerization curve to paclitaxel, GTP, $TPPS_4$ and PPIX rates (Eq.10).

$$S_1(t)=\frac{\alpha t}{k+\beta t} \qquad \text{Eq. (10)}$$

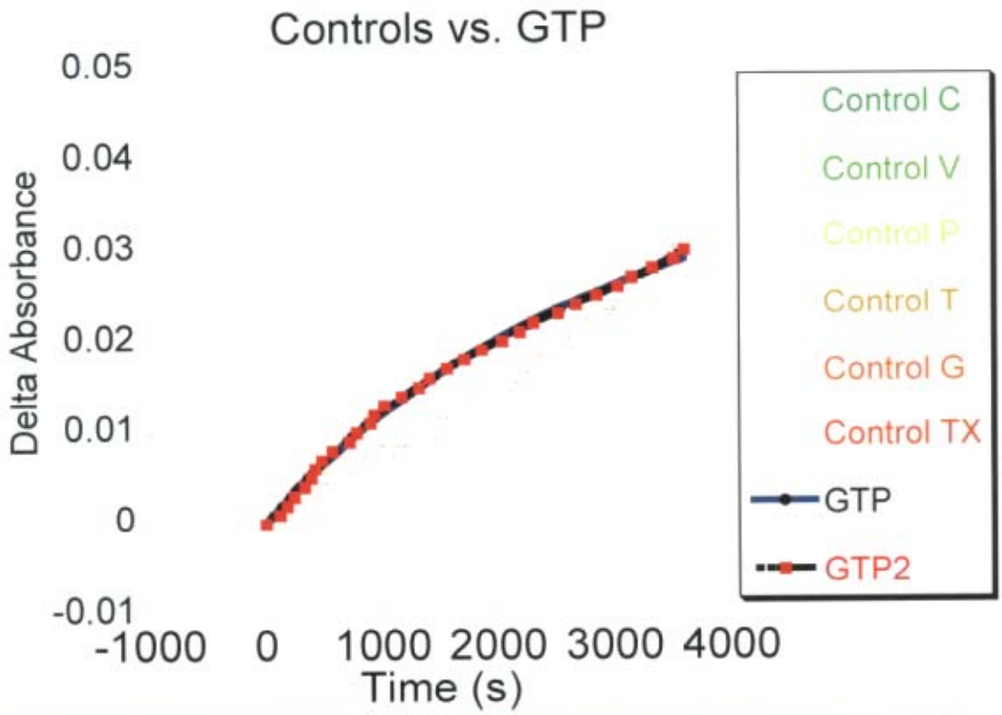
To further analyze the kinetics of tubulin polymerization a fitting of a two step polymerization curve was also performed (Eq.11).

$$S_2(t)=\frac{\alpha_1 t}{k_1+\beta_1 t}+\frac{\alpha_2 t}{k_2+\beta_2 t} \qquad \text{Eq. (11)}$$

Both of these fittings were calculated assuming certain weights for both α and β coefficients, where as k, k_1 *and* k_2 are the growth rate constants.

Sample	One Step(s^{-1})	Two Step (s^{-1})	
	k	K_1	k_2
Tubulin+GTP	55871	57076	32216
Tubulin+paclitaxel	27.255	2.5964	14.282
Tubulin+$TPPS_4$	1.8905e+05	9135.6	1.0013e+06
Tubulin+PPIX	80330	1291.5	66906

Table 2 Rate constants for tubulin polymerization.
These are the rate constants calculated with a one step and two step fitting. Notice the difference between the both porphyrins in there two step analysis.

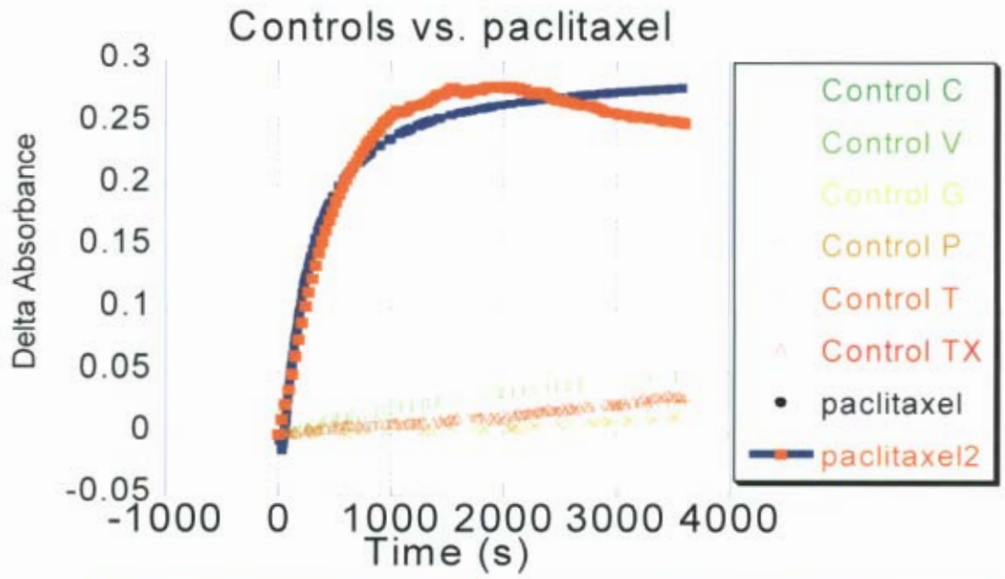


y = (m1*M0/(m2+m3*M0))		
	Value	Error
m1	0.82982	407.92
m2	55871	2.7477e+07
m3	12.952	6367.4
Chisq	5.6411e-06	NA
R	0.99887	NA

y = (m1*M0/(m2+m3*M0))+(m4*M...		
	Value	Error
m1	0.0036837	0.31449
m2	57076	4.3795e+06
m3	-14.278	1074.6
m4	0.49909	701.17
m5	32216	4.5281e+07
m6	9.0461	12706
Chisq	3.5763e-06	NA
R	0.99929	NA

Figure 18 GTP curve fit
This represents the curve fitting of GTP with a one step (left) and two step (right) polymerization fitting.

The growth rate constants found from the curve fittings indicate that our expectations were not meet (Table 2). The rate constants are inconsistent with our observations. GTP has a polymerization rate similar to tubulin alone, this indicates that the 10μM concentration was not large enough for the critical concentration of tubulin (Figure 18). However, it cannot be certain as to why paclitaxel had a low initial rate constant (Table 2).



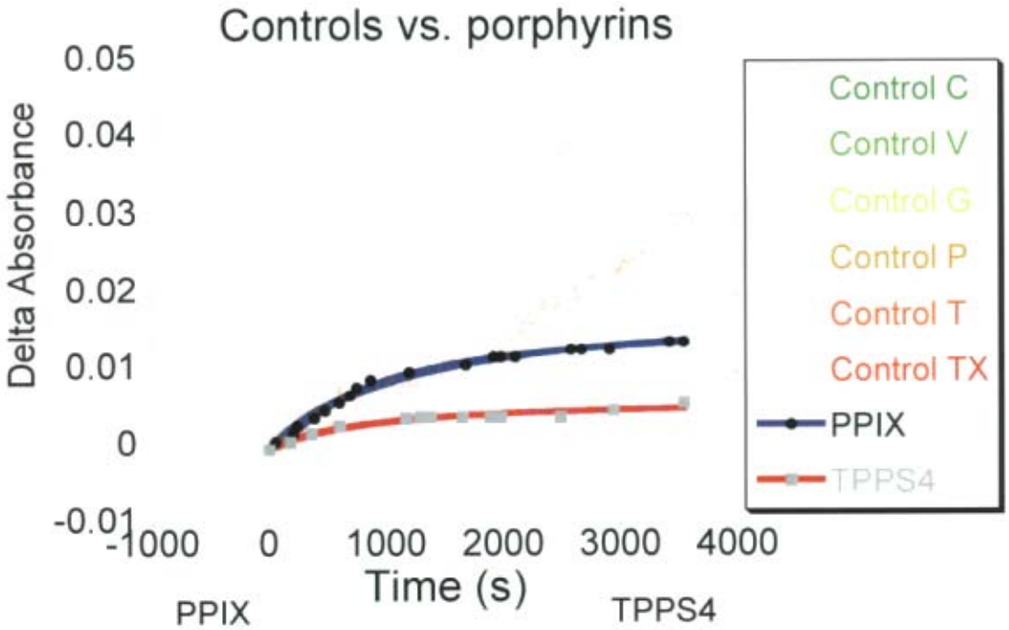
y = (m1*M0/(m2+m3*M0))		
	Value	Error
m1	0.027452	10.995
m2	27.255	10917
m3	0.089989	36.059
Chisq	0.04527	NA
R	0.95237	NA

y = (m1*M0/(m2+m3*M0))+(m4*M...		
	Value	Error
m1	0.39211	1651.3
m2	2.5964	4645.4
m3	0.029961	53.191
m4	-2.1891	9846.2
m5	14.282	48010
m6	0.17115	556.5
Chisq	0.031998	NA
R	0.96658	NA

Figure 19: Paclitaxel curve fit:
This represents the curve fitting of paclitaxel with a one step (left) and two step (right) polymerization fitting.

Although, it can be seen by the two step polymerization that paclitaxel has a very low initial growth rate constant followed by a larger secondary growth rate constant(Figure 19). According to Table 2, PPIX has a high initial growth rate constant which can also be observed in Figure 20. In the two step analysis PPIX seems to induce polymerization slowly then follows with a larger secondary growth rate constant similar to paclitaxel. According to our docking simulations (Figure 13), PPIX has the affinity to bind in the region close to that of GTP on β-tubulin. PPIX may have some effect on the binding of GTP, thus affecting the polymerization of tubulin. By our methods alone it cannot be certain that we are producing microtubule structures with this porphyrin. In this study we set out knowing that porphyrins bind to tubulin[19], however we're unsure as to how they may affect the polymerization of tubulin and also where they may bind to the structure. $TPPS_4$ showed a higher initial rate constant than PPIX. However, it is interesting to note that the growth rate constant behavior of the two step analysis is similar to paclitaxel. $TPPS_4$ has a lower initial growth rate constant (k_1) followed by a higher secondary growth rate constant (k_2). Thus it could be plausible to say that $TPPS_4$ may hyper-stabilize the polymerized structure to some extent.

In the background of paclitaxel the other ligands seem that they produce no polymerization(Figure 21). It is important to take note of the scales at which each graph is being represented on. Each ligand however is noticeably different than tubulin alone. Each ligand seems to have a unique turbidity signal, which leads us to believe that they have a unique mechanism for binding.



PPIX

y = (m1*M0/(m2+m3*M0))		
	Value	Error
m1	1.2888	666.96
m2	80330	4.1582e+07
m3	68.323	35368
Chisq	3.6003e-06	NA
R	0.99559	NA

TPPS4

y = (m1*M0/(m2+m3*M0))		
	Value	Error
m1	1.4568	2036.6
m2	1.8905e+05	2.6433e+08
m3	226.09	3.1618e+05
Chisq	1.8909e-06	NA
R	0.97068	NA

1 step

y = (m1*M0/(m2+m3*M0))+(m4*M...		
	Value	Error
m1	-1.5924	30368
m2	1291.5	1.3122e+07
m3	3.1552	30621
m4	82.763	1.1972e+06
m5	66906	3.012e+08
m6	158.58	6.9418e+05
Chisq	2.1715e-06	NA
R	0.99734	NA

y = (m1*M0/(m2+m3*M0))+(m4*M...		
	Value	Error
m1	0.12771	3.8639e+05
m2	9135.6	2.7875e+10
m3	10.923	2.0453e+07
m4	-6.2822	1.1364e+07
m5	1.0013e+06	1.099e+12
m6	1197	1.1181e+10
Chisq	1.8909e-06	NA
R	0.97068	NA

2 step

Figure 10: Porphyrin curve fitting
These curve fittings represent the one-step, and two-step polymerization for each porphyrin.

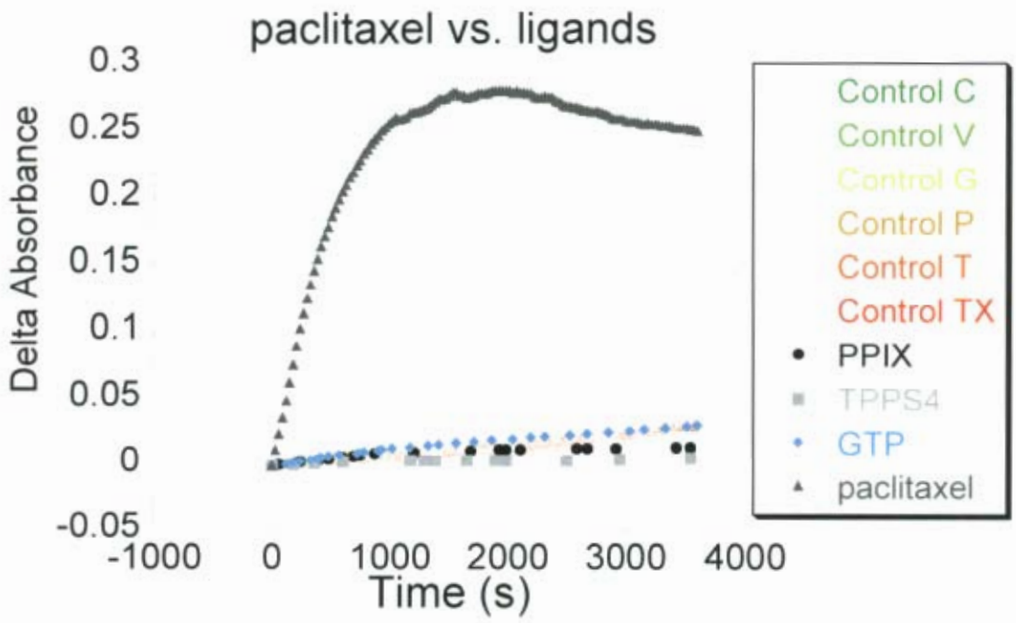


Figure 11: Paclitaxel vs. ligands
This is the comparison between paclitaxel and the tubulin alone (controls) and also tubulin with each ligans

According to our docking simulations, $TPPS_4$ has the affinity to bind in the region of paclitaxel, GTP, and Trp 21 on the β-tubulin. This gives even more support for the suggestion that $TPPS_4$ may have a similar effect as paclitaxel on tubulin polymerization. As for the overall structure that is produced, this cannot be certain with this measurement alone. Thus for both porphyrins the forming of aggregates or planar sheets of tubulin is also possible.

Future Direction:

In light of this research we would like to further investigate the formation of these polymerized structures of tubulin by both porphyrins using electron microscopy. We this we may be able to characterize what we are actually forming and thus give more support to our kinetic analysis of our polymerization rates. With an electron microscope we can

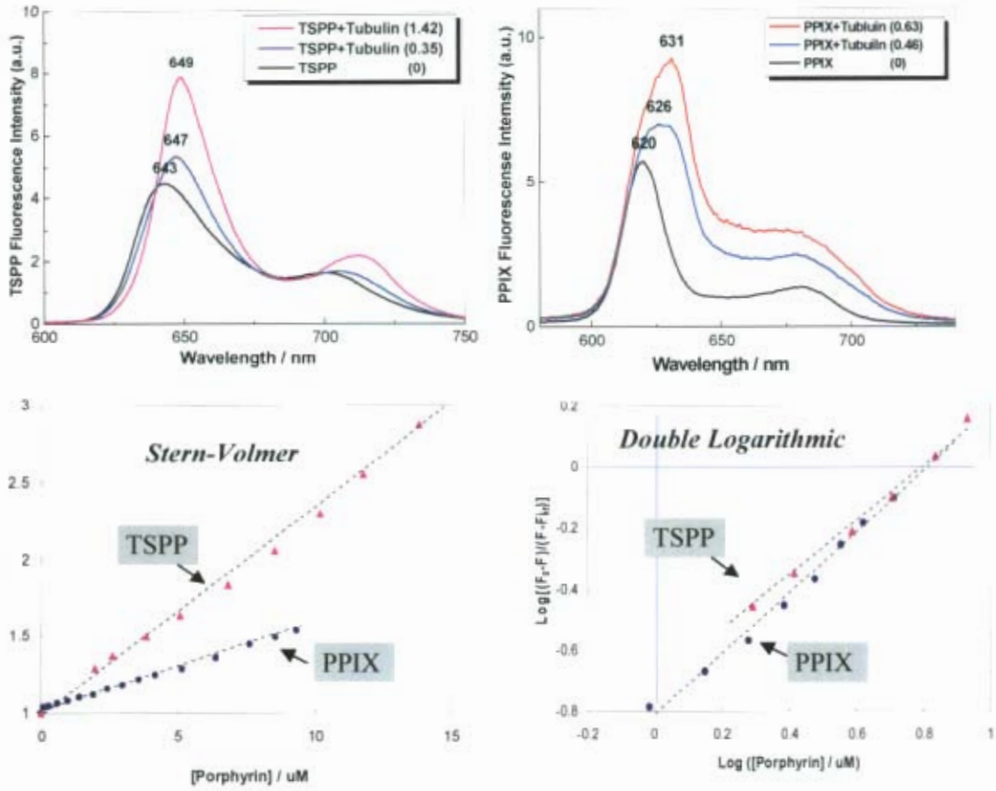
have a detailed image of what were are forming as well as the length and diameter of our possible microtubule structures. In addition we would also like to perform fluorescence correlation spectroscopy which will also be able to further characterize our formed structures by focusing on a fixed volume of solution and measuring the time that structures pass through this medium and to what extent. Also to understand the competition between each ligand and both porphyrins, we will induce polymerization of tubulin with each ligand then subject it to the addition of either $TPPS_4$ or PPIX and vice a versa.

References

[1] D.B. Min and J.M. Boff, Comphehensive Reviews in Food Science and Food Safety 1 (2002) 58-61.
[2] R. Aasland. (tubulin-dimer.jpg, ed.), Vol. 340 x 323, Bergen 2000.
[3] B. Vileno, M.g. Lekka, A. Sienkiewicz, P. Marcoux, A.J. Kulik, S. Kasas, S. Catsicas, A. Graczyk and L.a.o. Forr'o, J. Phys.: Condens. Matter 17 (2005) S1471–S1482.
[4] Y. Han, H. Malak, A.G. Chaudhary, M.D. Chordia, D.G. Kingston and S. Bane, Biochemistry 37 (1998) 6636-44.
[5] K. Boekelheide, J. Eveleth, A.H. Tatum and J.W. Winkelman, Photochem Photobiol 46 (1987) 657-61.
[6] M.F. Carlier and D. Pantaloni, Biochemistry 22 (1983) 4814-22.
[7] M.C. Wani, H.L. Taylor, M.E. Wall, P. Coggon and A.T. McPhail, J Am Chem Soc 93 (1971) 2325-7.
[8] M.A. Awan and S.A. Tarin, Surgeon 4 (2006) 231-6.
[9] C. Schweitzer and R. Schmidt, Chem Rev 103 (2003) 1685-757.
[10] T.J. Dougherty, Photochem Photobiol 58 (1993) 895-900.
[11] A.W. Girotti, Photochem Photobiol 51 (1990) 497-509.
[12] R.J. Fiel, N. Datta-Gupta, E.H. Mark and J.C. Howard, Cancer Res 41 (1981) 3543-5.
[13] J. Avila, Faseb J 4 (1990) 3284-90.
[14] K.H. Downing, Nogales, E., Curr. Op. Struct. Biol. 8 (1998) 785-791.
[15] E. Nogales, M. Whittaker, R.A. Milligan and K.H. Downing, Cell 96 (1999) 79-88.
[16] L.A. Amos, Lowe, J., Chem. Biol. 6 (1999) R65-R69.
[17] N. Yan and Y. Shi, Annu Rev Cell Dev Biol 21 (2005) 35-56.
[18] K. Berg and J. Moan, Photochem Photobiol 65 (1997) 403-9.
[19] F. Tian, E.M. Johnson, M. Zamarripa, S. Sansone and L. Brancaleon, Biomacromolecules 8 (2007) 3767-3778.
[20] D. Hall, Biophys Chem 104 (2003) 655-82.
[21] D. Hall and A.P. Minton, Anal Biochem 345 (2005) 198-213.
[22] K.E. Van Holde, W.C. Johnson and P.S. Ho, Principles of physical biochemistry, 2nd ed., Pearson/Prentice Hall, Upper Saddle River, NJ, 2006.
[23] C.R. Cantor and P.R. Schimmel, Biophysical chemistry, W. H. Freeman, San Francisco, 1980.
[24] F. Tian, K. Johnson, A.E. Lesar, H. Moseley, J. Ferguson, I.D. Samuel, A. Mazzini and L. Brancaleon, Biochim Biophys Acta 1760 (2006) 38-46.
[25] A. Lambier and Y. Engelborghs, Eur J Biochem 109 (1980) 619-24.
[26] S. Rao, Orr., G.A., Chaudahary, A.G., Kingston, D.G.I., Horwitz, S.B., J. Biol. Chem. 270 (1995) 20235-20238.

Appendix

A.1



	K_s / $^{5}M^{-1}$	n	K_d / ^{-6}M
TSPP	**1.7 ±**	**0.81 ± 0.10**	**4.9 ± 1.2**
PPIX	**0.54 ± 0.03**	**0.85 ± 0.06**	**6.0 ± 1.2**

*K_s: static quenching constant; n: binding sites; $_d$: dissociate

Fluorescence emission (above):

This is the fluorescence emission peaks of TSPP and PPIX upon the addition of tubulin. Notice the increase in intensity and red shifts demonstrating that binding is occurring.

Stern-Volmer* and *Double Logarithmic Plots (below)

Static quenching of tubulin fluorescence upon addition of TSPP and PPIX. The Stern-Volmer shows that TSPP has a larger rate for quenching. The double logarithmic plot indicates that they both have a binding site (~1).

A.2

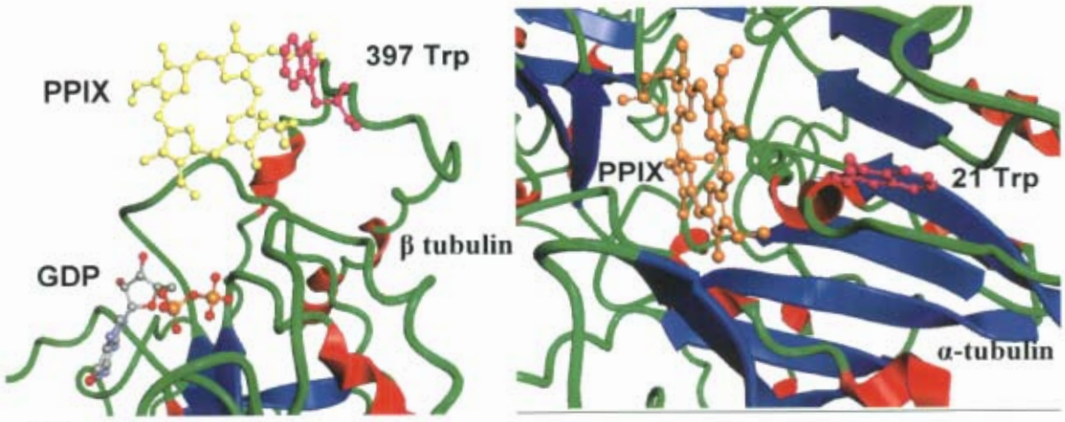
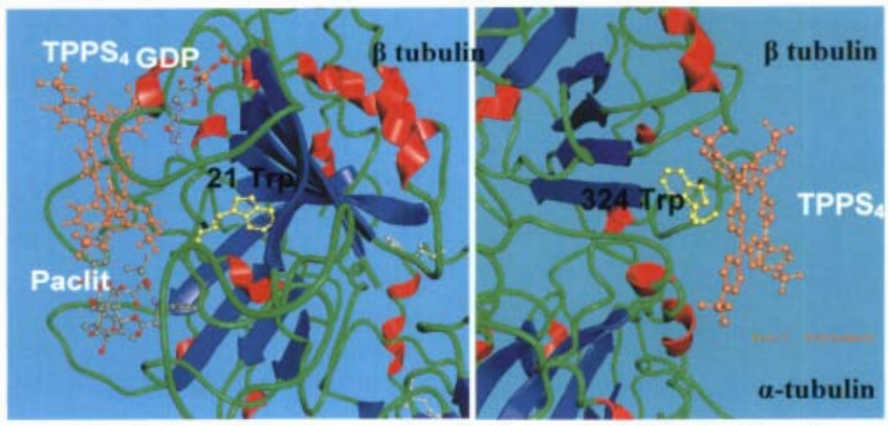


Figure 6:
PPIX: Yellow
Trp: Violet
GDP: CPK

These are simulations of PPIX binding to a tubulin dimer. PPIX has a binding energy of -11.2 kcal/mol when docked to 397 Trp located on β tubulin (left). PPIX has a binding energy of -10.5 kcal/mol when docked to 21 Trp located on α-tubulin (right).



TSPP: Orange
Trp: Yellow
GDP: CPK
Paclitaxel: CPK

These are simulations of $TPPS_4$ binding to a tubulin dimer. $TPPS_4$ has a binding energy of -10.1 kcal/mol when docked to 21 Trp located on β tubulin (left). $TPPS_4$ has a binding energy of -6.83 kcal/mol when docked to 324 Trp located on β tubulin (right).